OSTEOARTHRITIS

Mohawk is a transcription factor that promotes meniscus cell phenotype and tissue repair and reduces osteoarthritis severity

Kwang Il Lee[1], Ramya Gamini[1], Merissa Olmer[1], Yasunari Ikuta[1], Joe Hasei[1], Jihye Baek[1,2], Oscar Alvarez-Garcia[1], Shawn P. Grogan[1,2], Darryl D. D'Lima[1,2], Hiroshi Asahara[1], Andrew I. Su[3], Martin K. Lotz[1]*

Meniscus tears are common knee injuries and a major osteoarthritis (OA) risk factor. Knowledge gaps that limit the development of therapies for meniscus injury and degeneration concern transcription factors that control the meniscus cell phenotype. Analysis of RNA sequencing data from 37 human tissues in the Genotype-Tissue Expression database and RNA sequencing data from meniscus and articular cartilage showed that transcription factor Mohawk (MKX) is highly enriched in meniscus. In human meniscus cells, MKX regulates the expression of meniscus marker genes, OA-related genes, and other transcription factors, including Scleraxis (*SCX*), SRY Box 5 (*SOX5*), and Runt domain-related transcription factor 2 (*RUNX2*). In mesenchymal stem cells (MSCs), the combination of adenoviral MKX (Ad-MKX) and transforming growth factor–β3 (TGF-β3) induced a meniscus cell phenotype. When Ad-MKX–transduced MSCs were seeded on TGF-β3–conjugated decellularized meniscus scaffold (DMS) and inserted into experimental tears in meniscus explants, they increased glycosaminoglycan content, extracellular matrix interconnectivity, cell infiltration into the DMS, and improved biomechanical properties. Ad-MKX injection into mouse knee joints with experimental OA induced by surgical destabilization of the meniscus suppressed meniscus and cartilage damage, reducing OA severity. Ad-MKX injection into human OA meniscus tissue explants corrected pathogenic gene expression. These results identify MKX as a previously unidentified key transcription factor that regulates the meniscus cell phenotype. The combination of Ad-MKX with TGF-β3 is effective for differentiation of MSCs to a meniscus cell phenotype and useful for meniscus repair. MKX is a promising therapeutic target for meniscus tissue engineering, repair, and prevention of OA.

INTRODUCTION

Meniscus tears are the most common injury of the knee joint (*1*, *2*) and are, in many cases, associated with acute anterior cruciate ligament (ACL) lesions (*3*–*5*). Meniscus tears, particularly the most prevalent forms that occur in the avascular inner third, typically do not spontaneously heal and represent a major risk factor for knee osteoarthritis (OA) (*6*, *7*). Repair in the avascular region appears to require the recruitment and proliferation of resident cells, and their fibrochondrocytic differentiation is essential to restoring proper meniscus biomechanical function.

Delivery of individual biological factors or their combinations has been applied to promote meniscus regeneration in the avascular region. Transforming growth factor–β3 (TGF-β3) and basic fibroblast growth factor enhanced protein and glycosaminoglycan deposition in meniscus cells (*8*, *9*). Connective tissue growth factor (CTGF) directed fibroblast differentiation of endogenous stem/progenitor cells, and subsequent application of TGF-β3 was effective for fibrochondrocytic differentiation in vitro and in vivo (*10*, *11*).

Which transcription factors (TFs) govern the development and maintenance of the meniscus cell phenotype remains an unresolved question in meniscus cell biology, meniscus regeneration, and repair. Here, we used RNA sequencing (RNA-seq) data from the Genotype-Tissue Expression (GTEx) database (*12*, *13*), which includes data from 237 individuals, representing 43 sites and 37 different tissues. Meniscus and cartilage are not included in the GTEx data. We generated RNA-seq data from normal human knee meniscus and cartilage to perform a genome-wide identification of meniscus-enriched (ME) genes and TFs that potentially control their expression. We found that the TF Mohawk (MKX) was highly enriched in meniscus. We analyzed whether MKX regulates the meniscus cell phenotype and can be applied for meniscus repair and prevention of OA in vivo.

RESULTS

MKX is an ME TF

To determine which TFs are expressed and enriched in human meniscus, we used the GTEx database, which contains RNA-seq data from 37 different human tissues and 43 different sites (*12*, *13*). Because meniscus and other joint tissues are not represented in GTEx, we generated RNA-seq data from normal human meniscus and articular cartilage tissues that were obtained from postmortem donors without a history of joint disease or injury. We compared the expression values (logCPM) in the individual meniscus samples with the individual samples from all other tissues in GTEx to identify genes that are ME. We applied a stringent cutoff ($P < 0.01$ and $\log_2FC > 1$) and identified 472 ME genes. To determine which of the 472 ME genes are TFs, we used the Gene Ontology (GO) term "TF activity, sequence specific DNA binding" (GO: 0003700) (total $n = 1209$) (*14*). This identified 55 TFs that are enriched in meniscus

[1]Department of Molecular Medicine, Scripps Research, La Jolla, CA 92037, USA. [2]Shiley Center for Orthopaedic Research and Education at Scripps Clinic, La Jolla, CA 92037, USA. [3]Department of Integrative, Structural and Computational Biology, Scripps Research, La Jolla, CA 92037, USA.
*Corresponding author. Email: mlotz@scripps.edu

when comparing RNA-seq from meniscus with GTEx without cartilage (table S1) and 14 TFs when comparing meniscus with tissues in GTEx and cartilage (table S2). In this list of 14 TFs, the most ME TF, zinc finger 573 (*ZNF573*), is not well characterized (*15*). *MKX* is the second most ME TF and has higher expression (logCPM) in meniscus than in all tissues in GTEx and articular cartilage (Fig. 1A). The mRNA expression of *MKX* as reflected in RNA-seq count values was higher than for *ZNF573* (fig. S1A). *MKX*, *ZNF573*, and *ZNF765* had the highest RNA-seq count values in meniscus compared to GTEx and articular cartilage (fig. S1, B to D).

To confirm and extend the results from the RNA-seq experiments, we analyzed additional connective tissues by quantitative polymerase chain reaction (qPCR) of *MKX* mRNA in different human joint tissues and bone marrow–derived mesenchymal stem cells (BM-MSC). *MKX* mRNA expression in healthy meniscus was similar to normal ACL and higher than in normal articular cartilage, where *MKX* expression is similar among the different zones (fig. S2) (*16*). *MKX* mRNA expression in human BM-MSC was much lower than in the joint tissues (Fig. 1B). *MKX* expression in damaged OA meniscus was lower than in normal meniscus, and MKX expression in the normal vascular zone was higher than in the avascular zone (Fig. 1, C and D). These results indicate that *MKX* expression correlates with MSC differentiation to mature connective tissue cells, and *MKX* expression is suppressed in damaged meniscus.

MKX is a member of the Iroquois (IRX) gene family, which includes six *IRX* genes and *MKX* as an *IRX*-like gene. We analyzed the expression of *IRX* genes in the RNA-seq dataset and found that the expression of all *IRX* genes (log_2CPM) was much lower than *MKX* (Fig. 1E). Thus, *MKX* is a TF that is highly enriched in mature normal meniscus, suggesting that it is a previously unidentified transcriptional regulator of the meniscus cell phenotype.

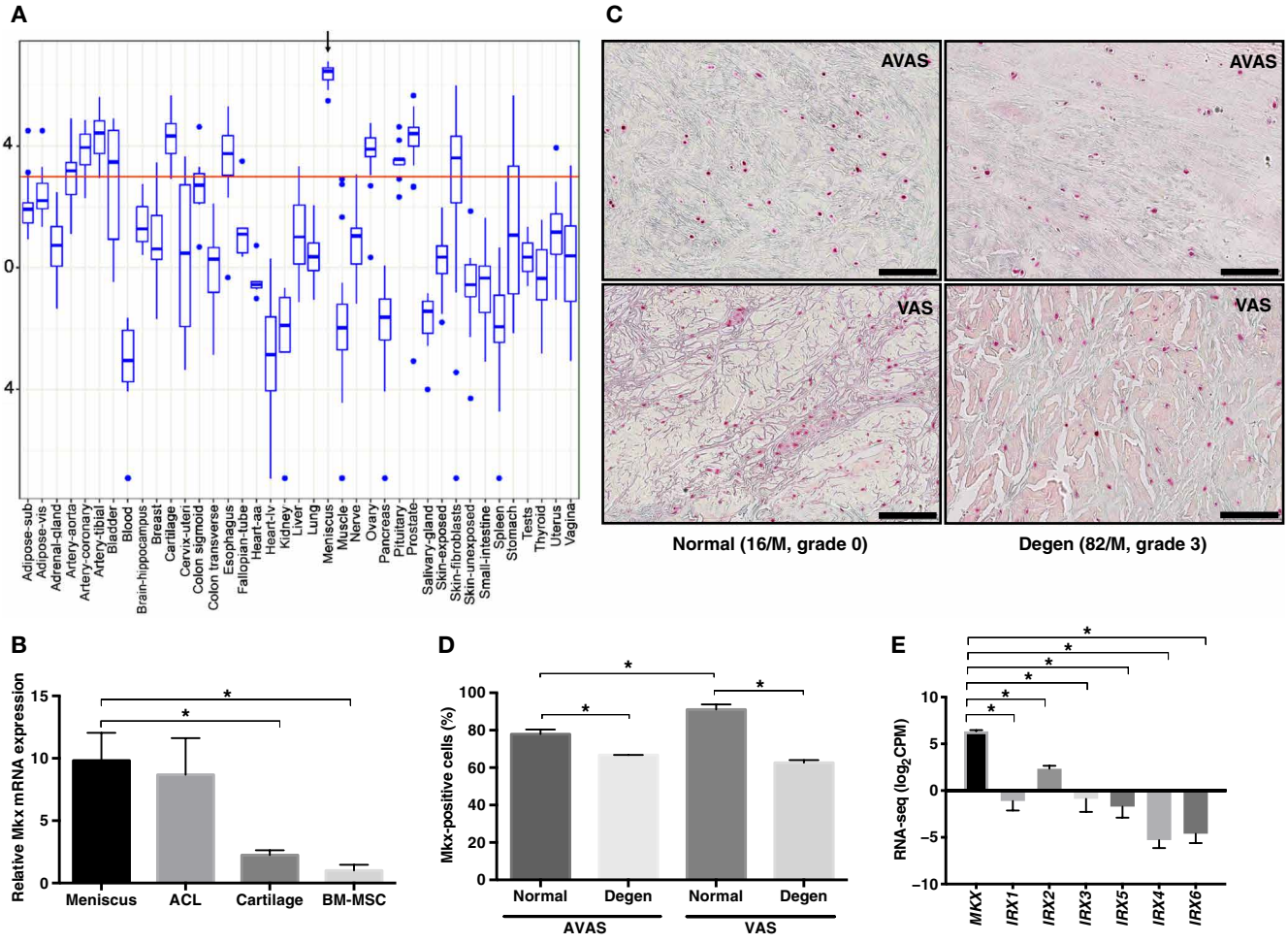

Fig. 1. *MKX* gene expression in meniscus. (**A**) *MKX* expression (arrow) compared to tissues in GTEx and RNA-seq data from meniscus and articular cartilage. Box plots are shown for *MKX* expression values (logCPM) in 37 tissues in GTEx and in meniscus and cartilage. (**B**) *MKX* expression in different joint tissues and BM-MSCs. Human knee joints from healthy donors were collected at autopsy and used for RNA isolation from ACL ($n = 8$), meniscus ($n = 7$), articular cartilage ($n = 6$), and human BM-MSCs ($n = 8$) from monolayer culture in basal media. qRT-PCR was performed for *MKX* and *GAPDH*. *$P < 0.05$ (one-way ANOVA) as compared to meniscus. (**C**) Immunohistochemistry of MKX in the avascular (AVAS) and vascular (VAS) region of healthy (16/M, grade 0) and degenerated (82/M, grade 3) human meniscus tissue. Scale bars, 100 μm. (**D**) MKX-positive cells were quantified for each avascular and vascular region of normal or degenerated human meniscus ($n = 4$ per group). *$P < 0.05$ (one-way ANOVA) compared to the selected groups. (**E**) RNA-seq analysis of Iroquois (*Irx*) family–related homeobox protein including MKX (Irx-like 1) from human meniscus ($n = 10$). *$P < 0.05$ (one-way ANOVA) as compared to *MKX*. All values are means ± SEM.

Meniscus-like cell differentiation of MSCs in response to MKX and TGF-β3

To study the role of MKX in MSC differentiation to a meniscus-like cell phenotype, we transduced MSCs with adenoviral MKX (Ad-MKX). We chose a multiplicity of infection (MOI) of 100 based on cell viability and *MKX* mRNA expression in Ad-MKX–transduced cells after 10 days in pellet culture (fig. S3, A and B). Ad-MKX–transduced cells showed higher mRNA expression of fibrogenic differentiation–related genes such as tenomodulin (*TNMD*), Tenascin C (*TNC*), *COL1A1*, and TF *SCX* than the control groups (fig. S3C). The cells transduced by Ad-GFP (green fluorescent protein) expressed green fluorescence in an MOI dose-dependent pattern (fig. S3D). We compared Ad-MKX with other factors including TGF-β3, bone morphogenetic protein 12 (BMP12), growth differentiation factor 5 (GDF5), and CTGF that regulate fibrogenic or chondrogenic markers that are also part of the meniscus cell phenotype (Fig. 2, A to E) and found that Ad-MKX–transduced MSCs expressed the highest *COL1A1*, *TNC*, and *TNXB*. The combination of Ad-MKX and TGF-β3 induced MSC differentiation to a phenotype that most closely resembled mature meniscus cells (Figs. 2, F to I, and 3, A and B). As previously reported (*17*), TGF-β3 induced the expression of chondrogenic markers (*COL2A1*) and proteoglycans [chondroadherin (*CHAD*), cartilage oligomeric matrix protein (*COMP*), decorin (*DCN*), and hypertrophic markers (*RUNX2*, *COL10A1*, and *MMP13*)] in MSC pellet culture (Fig. 3C). However, Ad-MKX reduced hypertrophic markers (Fig. 3D). The combination of Ad-MKX and TGF-β3 increased meniscus-specific markers such as COL1A1, COL2A1, and ACAN (Fig. 3, E and F). In synovial MSCs (SYN-MSCs) from human knee joints, Ad-MKX transduction had similar effects as in BM-MSCs (fig. S4). RNA-seq count values for *COL1A1*, *TNC*, and *TNMD* were higher in meniscus than articular cartilage, and the expression of *TNXB* in meniscus was similar to the expression of *COL1A1* (fig. S5). These results indicate that the combination of Ad-MKX and TGF-β3 induced MSC differentiation to a meniscus cell phenotype.

MKX regulation of gene expression in human meniscus cells

To assess MKX function in meniscus cells, we used Ad-MKX overexpression and small interfering RNA (siRNA)–mediated knockdown of *MKX* in cells from healthy human meniscus. In healthy avascular meniscus cells, Ad-MKX increased the expression of TF *SCX* and decreased *SOX5* and *RUNX2*. Ad-MKX suppressed the expression of genes related to meniscus degeneration [A disintegrin and metalloproteinase with thrombospondin motifs (*ADAMTS4*), *ADAMTS5*, *IL-6*, *MMP1*, and *MMP3*], hypertrophy (*RUNX2* and *COL10A1*), and calcification [ankylosis protein homolog (*ANKH*) and ectonucleotide pyrophosphatase/phosphodiesterase 1 (*ENPP1*)] (Fig. 4A). When we compared the gene expression between Ad-MKX–transduced

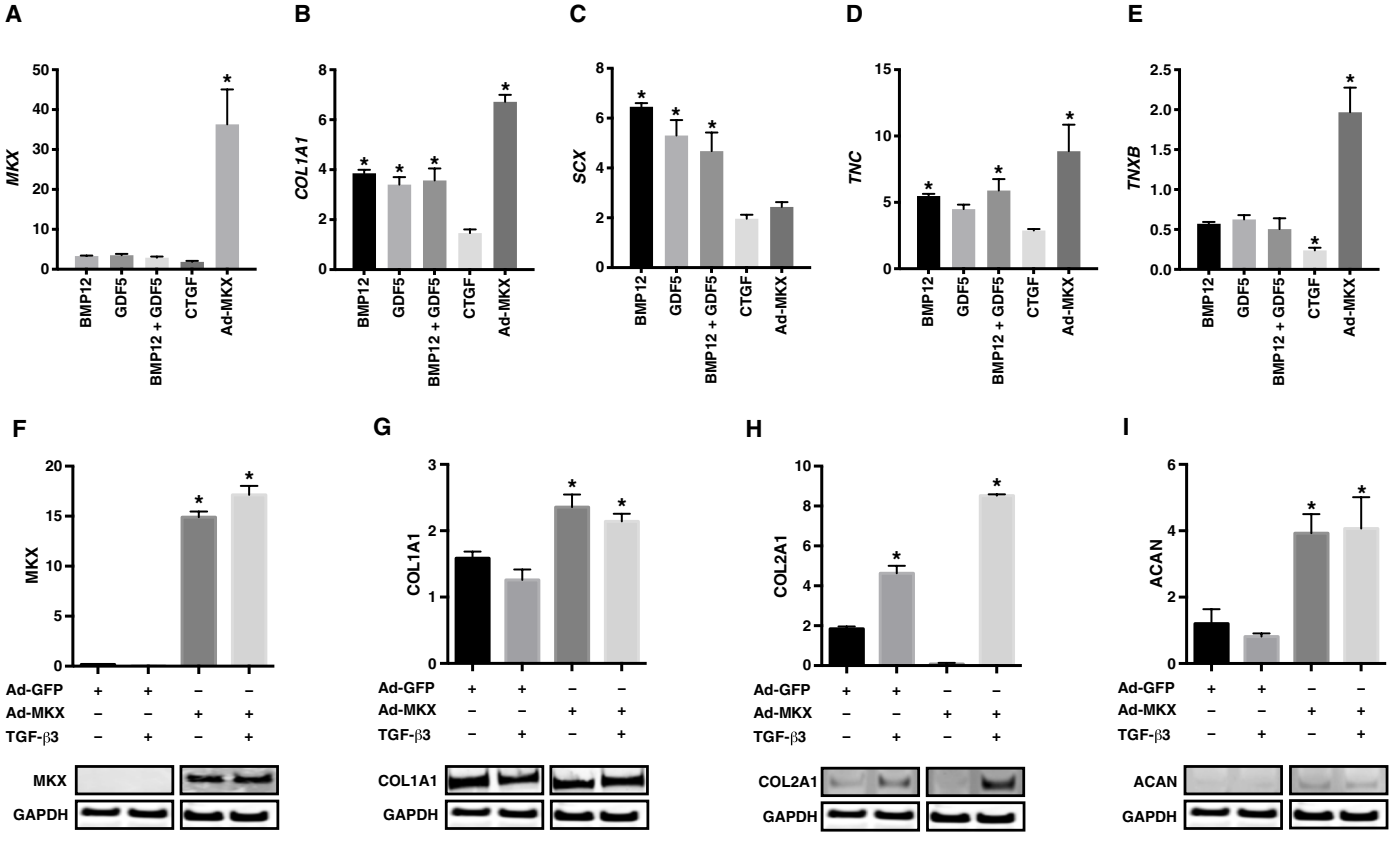

Fig. 2. Effects of growth factors and Ad-MKX on gene expression in MSCs. Human bone marrow–derived mesenchymal stem cells (BM-MSCs) ($n = 4$) were cultured with growth factors BMP12, GDF5, and CTGF (100 ng/ml). Ad-MKX–transduced BM-MSCs were cultured with basal media. RNA was isolated after 14 days for qRT-PCR analysis of (**A**) *MKX* (**B**) *COL1A1*, (**C**) *SCX*, (**D**) *TNC*, and (**E**) *TNXB*. *$P < 0.05$ (one-way ANOVA) as compared to BM-MSC that was normalized to 1. For analysis of protein expression, BM-MSCs ($n = 4$ for each condition) were cultured for 14 days for Western blotting analysis of (**F**) MKX, (**G**) COL1A1, (**H**) COL2A1, and (**I**) ACAN. *$P < 0.05$ (one-way ANOVA) as compared to Ad-GFP–transduced BM-MSCs. All values are means ± SEM.

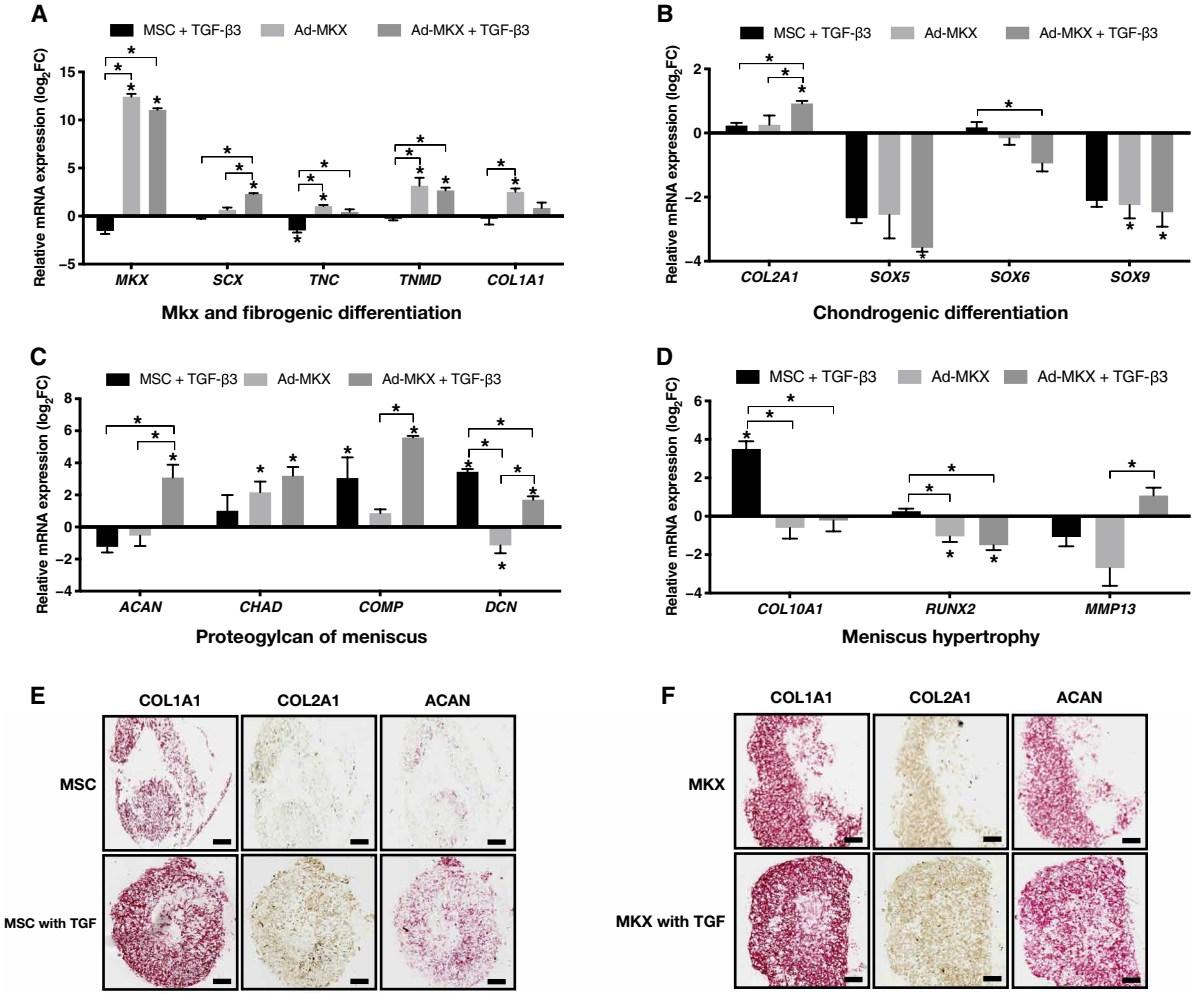

Fig. 3. Gene expression analysis and immunohistochemistry in BM-MSCs after Ad-MKX transduction and TGF-β3 stimulation. BM-MSC pellets ($n = 6$) cultured in media with chondrogenic supplements with or without TGF-β3 and with or without Ad-MKX (MOI, 100) transduction. RNA was isolated after 2 weeks and analyzed by qRT-PCR. Gene expression of (**A**) MKX and fibrogenic differentiation–related genes, (**B**) chondrogenic differentiation–related genes, (**C**) proteoglycan of meniscus-related genes, and (**D**) meniscus hypertrophy–related genes. Immunohistochemistry of COL1A1, COL2A1, and ACAN; (**E**) BM-MSC pellets in basal media and BM-MSC pellets in TGF-β3 media; and (**F**) Ad-MKX–transduced BM-MSC pellets in basal media and Ad-MKX–transduced BM-MSC pellets in TGF-β3 media. Results are from three to four separate experiments, each performed in duplicate. Gene expression was normalized by values in BM-MSC without Ad-MKX or TGF-β3. *$P < 0.05$ one-way ANOVA) as compared to the selected group. All values are means ± SEM. Scale bars, 100 μm.

vascular cells and Ad-MKX–transduced avascular cells, the only difference was that Ad-MKX suppressed *SOX9* in vascular cells but not in avascular cells. All other genes that were analyzed were similarly changed by Ad-MKX in both cell types (fig. S6A). MKX siRNA decreased *MKX* expression and increased *SOX5*, *SCX*, *MMP13*, *RUNX2*, and *ENPP1* in normal avascular meniscus cells (Fig. 4B). MKX siRNA increased *COL2A1*, but *COL1A1* and AGGRECAN (*ACAN*) were not changed (fig. S6B). However, Ad-MKX did not change *COL1A1*, *COL2A1*, or *ACAN* (fig. S6C). These results indicate that in human meniscus cells, MKX regulates not only the expression of meniscus-degenerative and calcification-related genes but also other TFs (*SCX*, *SOX5*, and *RUNX2*).

We also tested whether MKX affects the expression of genes that are involved in the pathogenesis of meniscus degeneration in normal and OA meniscus cells and in cells that were activated with the proinflammatory cytokine interleukin-1β (IL-1β). Ad-MKX suppressed genes related to OA (*ADAMTS5*, *IL-6*, *MMP1*, and *MMP3*), hypertrophy (*MMP13*, *RUNX2*, and *COL10A1*), and calcification (*ENPP1* and *ANKH*) in OA avascular meniscus cells (Fig. 4C). Ad-MKX also suppressed the IL-1β effect on these genes in OA avascular cells (Fig. 4D). These results indicate that MKX protects normal and OA meniscus cells against gene expression associated with degeneration, hypertrophy, calcification, and OA.

Ad-MKX–transduced MSCs on TGF-β3–coated decellularized meniscus scaffold promote healing of experimental meniscus tears ex vivo

We designed approaches to test whether Ad-MKX–transduced MSCs can be applied to promote healing of meniscus tears. We developed a bovine decellularized meniscus scaffold (DMS) (*18*) that was conjugated with heparin to enhance binding of growth factors and optimized it for retention of TGF-β3 (fig. S7). MSCs cultured on the

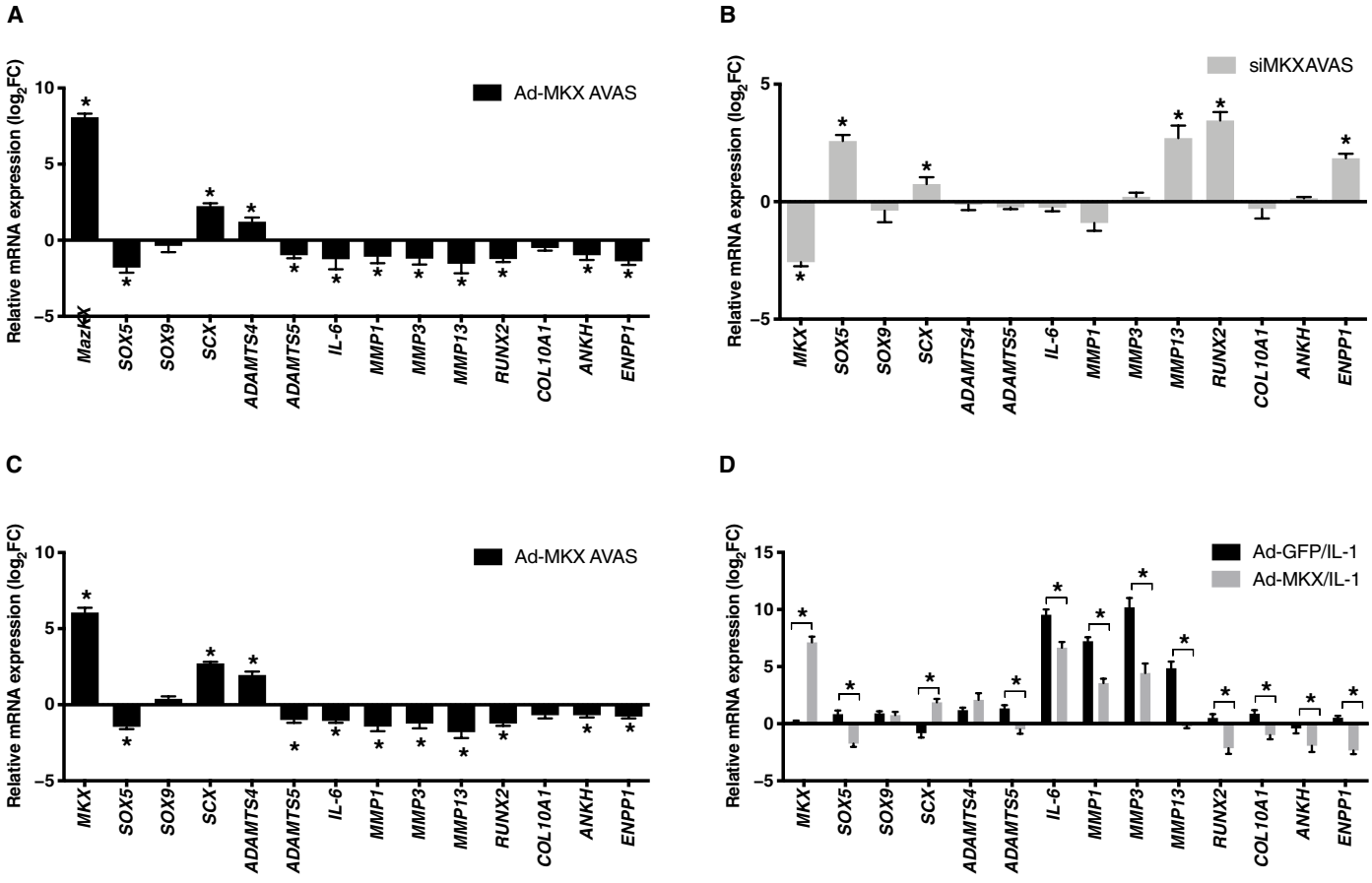

Fig. 4. Ad-MKX for overexpression and siRNA-mediated knockdown of MKX in meniscus cells. qRT-PCR analysis of genes related to meniscus degeneration, hypertrophy, and calcification at 48-hour posttransduction of meniscus cells ($n = 6$ to 10) with Ad-MKX or MKX siRNA. (**A**) Ad-MKX transduction of normal avascular cells. *$P < 0.05$ (one-way ANOVA) as compared to Ad-GFP–transduced healthy avascular cells. (**B**) siRNA MKX transduction of normal avascular cells. *$P < 0.05$ (one-way ANOVA) as compared to siRNA control–transduced normal avascular cells. (**C**) Ad-MKX transduction of OA avascular cells. *$P < 0.05$ (one-way ANOVA) as compared to Ad-GFP–transduced OA avascular cells. (**D**) Ad-MKX transduction of OA avascular cells with IL-1β (0.5 ng/ml). *$P < 0.05$ (one-way ANOVA) as compared to Ad-GFP–transduced OA avascular cells with IL-1β (0.5 ng/ml) after being normalized by Ad-GFP–transduced OA avascular cells without IL-1β. All values are means ± SEM.

TGF-β3–conjugated DMS showed higher cell proliferation compared with the other groups (fig. S8, A to C). DAPI (4′,6-diamidino-2-phenylindole) staining after 2 weeks of ex vivo culture showed higher cell density in the heparin-conjugated DMS and TGF-β3–conjugated DMS (fig. S8, D to F).

As an experimental model, we used live bovine meniscus explants with surgically induced meniscus tears (*19*–*21*). Various preparations of DMS were inserted into the tears, including DMS only, MSCs on DMS, MSCs on TGF-β3–conjugated DMS, Ad-MKX–transduced MSCs on DMS, and Ad-MKX–transduced MSCs on TGF-β3–conjugated DMS. After 2 weeks of ex vivo culture, the highest Safranin-O staining intensity and the largest number of DAPI-positive cells in the DMS and on the surface of DMS were observed in the group with Ad-MKX–transduced MSCs on the TGF-β3–conjugated DMS (Fig. 5, A to C). Safranin-O staining intensity and DAPI-positive cells in the DMS were higher in heparin- and TGF-β3–conjugated DMS, which correlates with higher ACAN expression in Ad-MKX–transduced MSC pellets cultured with TGF-β3 and increased cell density in MSC on heparin-conjugated DMS and heparin with TGF-β3–conjugated DMS. There was a synergistic effect of Ad-MKX overexpression and TGF-β3 in Safranin-O intensity and numbers of infiltrated cells. Polarized picrosirius red staining and differential interference contrast (DIC) microscopy showed the highest interconnectivity between DMS and injured bovine explant in the group with Ad-MKX–transduced MSCs on TGF-β3–conjugated DMS, and this group also showed collagen fiber alignment at the interface (Fig. 5D). Young's modulus, a biomechanical property determined by tensile testing, was highest in the Ad-MKX MSCs and TGF-β3 group (Fig. 5E).

MKX protects against meniscus and cartilage damage in vivo

To test the therapeutic potential of MKX in vivo, we used an experimental model with surgical destabilization of the medial meniscus (DMM), which features severe meniscus damage and cartilage degradation characteristic of OA (*22*). After 4 weeks from the first Ad-GFP or Ad-MKX injection into the mouse knee joints, histopathology was evaluated by using Safranin-O staining images (fig. S9, A to D). Ad-MKX–injected mouse knee joint was used as a negative control, indicating that green fluorescence was not detected in menisci and articular cartilage (fig. S9E). After Ad-GFP injection into nonsurgical mouse knee joints, fluorescence was detected in nonsurgical menisci and articular cartilage after 4 weeks from the first injection (fig. S9F).

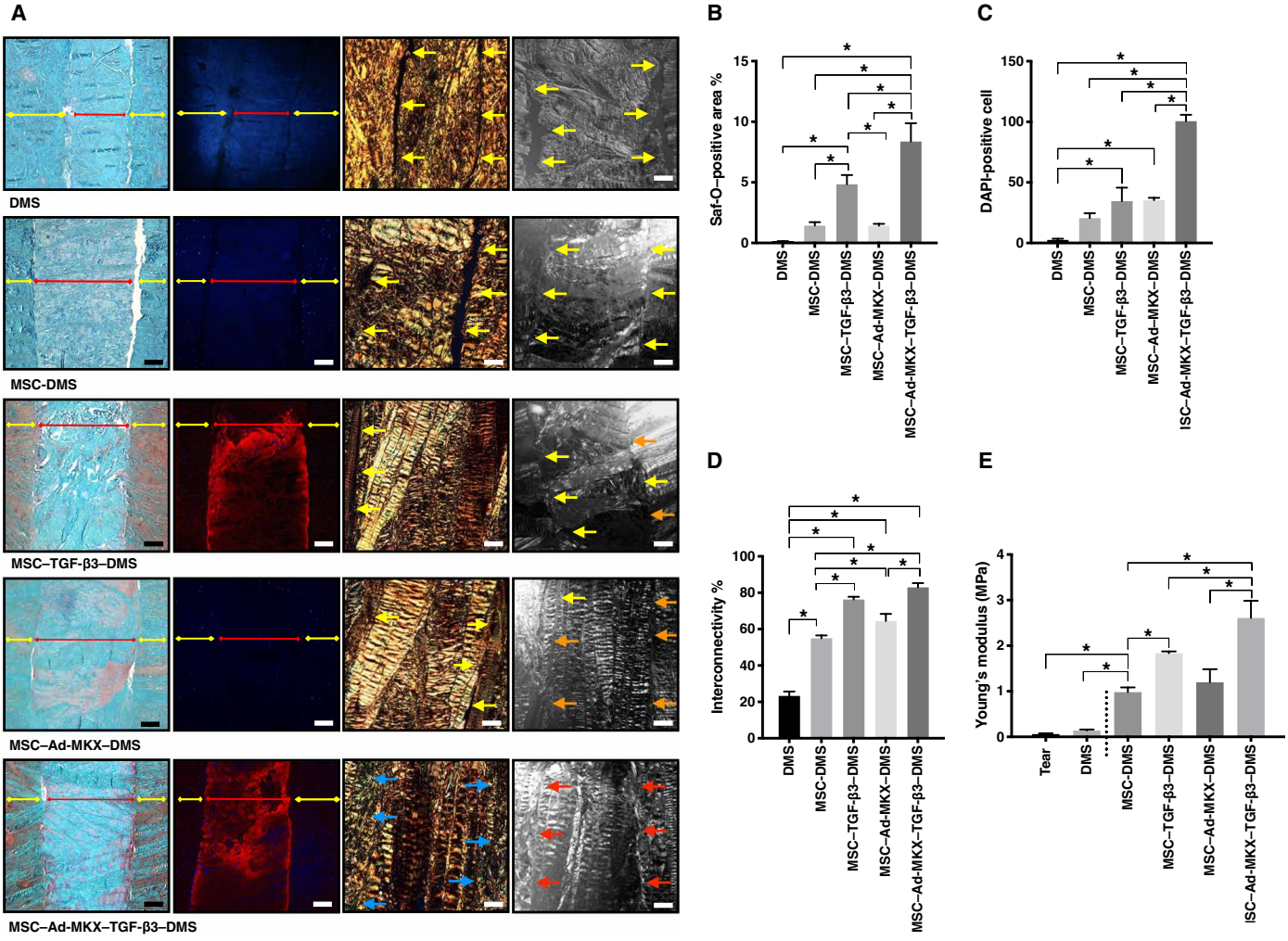

Fig. 5. MKX in the treatment of experimental tears in meniscus explants. Experimental tears in bovine meniscus explants ($n = 4$) were inserted with various preparations of DMS and cultured for 2 weeks. Groups included DMS only, MSCs on DMS, MSCs seeded on TGF-β3–coated DMS, Ad-MKX–transduced MSCs seeded on DMS, and Ad-MKX–transduced MSCs seeded on TGF-β3–coated DMS. (**A**) Tissue sections were stained with Safranin-O, DAPI, picrosirius red with polarized light, and differential interference contrast (DIC) imaging. Double-headed arrows in Safranin-O and DAPI stain indicate tissue identity. Yellow, bovine meniscus explant; red, conditional DMS. The red fluorescence represents TGF-β3. Arrows in picrosirius red stain and DIC images indicate tissue connectivity conditions. Yellow, nonconnected area; orange, connected area with visible borderline; red, connected area and covered with fibers, which is shown as white lines; blue, type III collagen fibers, which is indicated as a green polarized color covering the borderline. (**B**) The Safranin-O–positive area in the DMS was detected by analyzing the threshold color and total area and was calculated using ImageJ. The percent Safranin-O–positive area was calculated. (**C**) DAPI-positive cells in the DMS were counted, and cell counts were normalized by the DMS and DMS/meniscus interface area that was analyzed. (**D**) The area of the meniscus/DMS interface that was connected by collagen fibers was measured and expressed as % interconnectivity. Meniscus explants with experimental tears were inserted with various DMS preparations as indicated and cultured for 4 weeks. (**E**) Tensile testing ($n = 6$) was performed and calculated with Young's modulus. Data represent a minimum of three separate experiments, where each condition was tested in eight replicates. *$P < 0.05$ (one-way ANOVA) as compared to the selected group. All values are means ± SEM. Scale bars, 100 μm.

In joints with DMM, cells from the vascular region of meniscus and from the synovium had migrated to the damaged outer meniscus surface, and these cells were fluorescent (fig. S9G). The most severely damaged menisci also showed strong fluorescence inside meniscus tears where cells had infiltrated (fig. S9H). In sham-control mouse knee joints injected with Ad-GFP or Ad-MKX, MKX expression was observed mostly in synovium and meniscus vascular zone (fig. S10, A to F, black arrows). However, in joints with DMM, MKX expression was seen in the entire meniscus (fig. S10, G to J, black arrows). Anterior meniscus degeneration in male mice was more severe than in female mice (Fig. 6A and fig. S11, A and B). Ad-MKX injection resulted in less severe degenerative changes in anterior meniscus in female mice and less severe changes in the posterior meniscus in both male and female mice (Fig. 6, B and C, and fig. S11, C and D). Combining data from male and female mice, Ad-MKX reduced meniscus histopathology scores in anterior and posterior meniscus (Fig. 6D). Ad-MKX also reduced articular cartilage histopathology scores in both female and male mice (Fig. 6, E to G). Furthermore, Ad-MKX reduced synovium histopathology scores (Fig. 6H). COL10A1 and RUNX2 were suppressed by Ad-MKX to almost undetectable expression. Menisci in Ad-MKX–injected mouse joints did not change COL1A1 and COL2A1 expression compared with

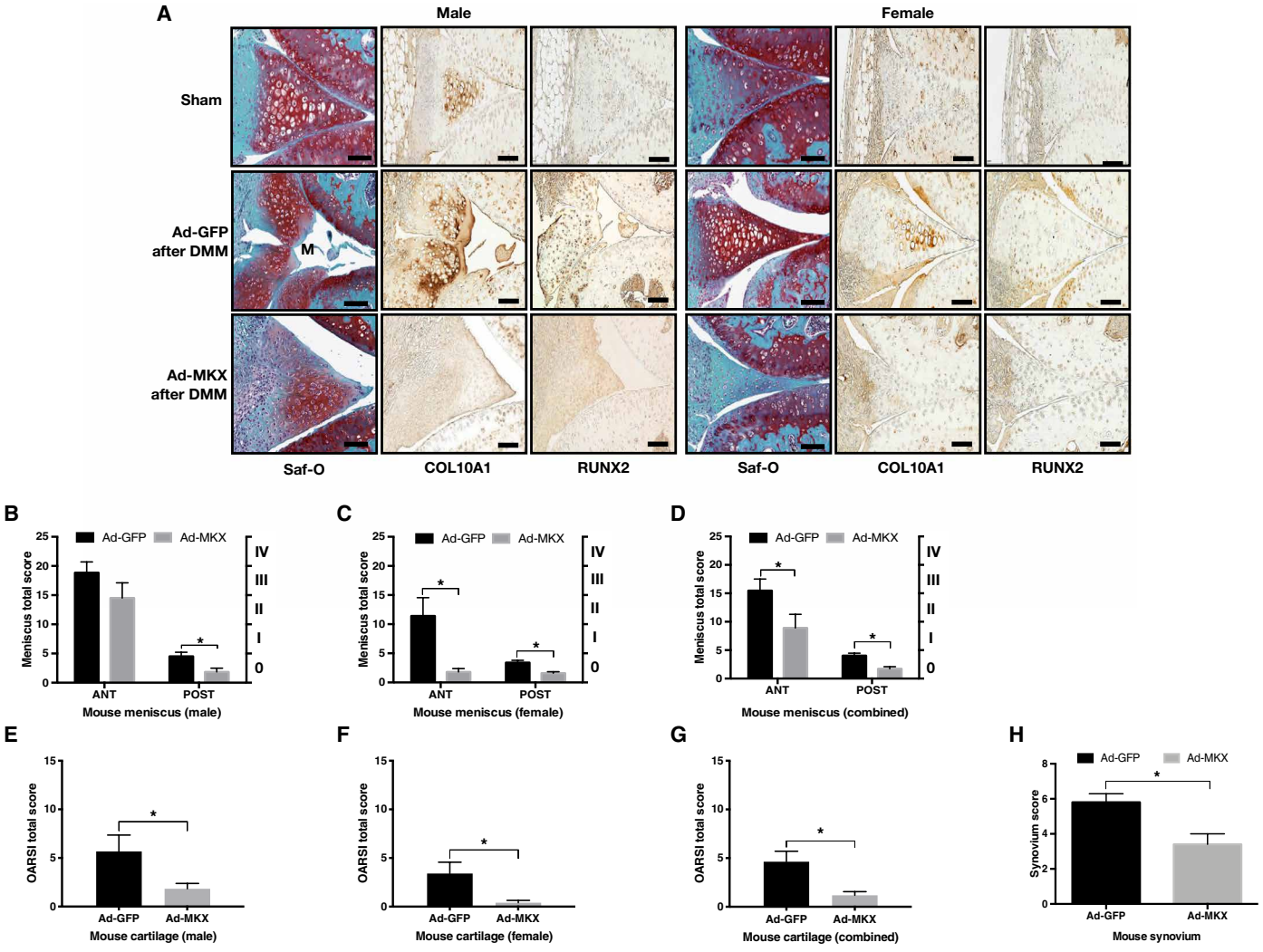

Fig. 6. Ad-MKX injection into mouse knee joints after DMM surgery. Ad-GFP or Ad-MKX virus (1×10^{10} pfu/ml) was injected into the mouse knee joint ($n = 11$; 6 males and 5 females) at 1 week after DMM surgery. The same amount (10 μl) of virus was injected once per week for 4 weeks. (**A**) Safranin-O staining and immunohistochemistry (COL10A1 and RUNX2) of the mouse knee joint (anterior region) from sham surgery, Ad-GFP–injected knee joint with DMM surgery, and Ad-MKX–injected knee joint with DMM surgery after 4 weeks. "M" indicates the degenerative anterior meniscus in male mice. Meniscus histopathological score was calculated for (**B**) male and (**C**) female mice, and (**D**) total scores were compared. Osteoarthritis Research Society International (OARSI) articular cartilage score was calculated for (**E**) male and (**F**) female mice, and (**G**) total scores were compared. (**H**) Synovium scores. *$P < 0.05$ (Mann-Whitney test) as compared to the Ad-GFP–injected mice group. All values are means ± SEM. Scale bars, 100 μm.

the sham group; however, mouse menisci from joints with DMM surgery and Ad-GFP injection showed abnormal COL2A1 expression in the vascular region associated with hypertrophic changes (fig. S12).

Ad-MKX injection promotes healing of human OA meniscus ex vivo

To test the potential of MKX to have therapeutic benefit in human tissues, meniscus explants from patients with OA were infected with Ad-MKX. Meniscus histopathology scores were improved by Ad-MKX (Fig. 7, A and B, and fig. S13). Immunohistochemistry showed that Ad-MKX reduced markers of chondrocyte hypertrophy (MMP13, COL10A1, and RUNX2) (Fig. 7C). Gene expression analysis showed that Ad-MKX injection also reduced the expression of genes related to hypertrophic differentiation (*MMP13*, *COL10A1*, and *RUNX2*), extracellular matrix (ECM) degradation (*ADAMTS5*), and calcification (*ANKH* and *ENPP1*) without changes in meniscus ECM genes (*COL1A1*, *COL2A1*, and *ACAN*) (Fig. 7D).

DISCUSSION

In this study, we identified MKX as a meniscus-expressed and highly enriched TF and tested it for its potential to regulate meniscus cell phenotype, to direct meniscus cell differentiation of MSC, to promote healing of meniscus tears, and to attenuate the consequences of meniscus injury in vivo. Only a limited number of TFs have been examined for expression and function in meniscus. Early growth response 1 (*EGR1*), a mediator of TGF-β3–induced fibrosis (*23*), showed the largest differential expression in the meniscus versus cruciate ligaments during mouse embryonic development (*24*). *EGR1* is involved in vertebrate tendon differentiation by regulating type I collagen production (*25*). To determine on a genome-wide expression

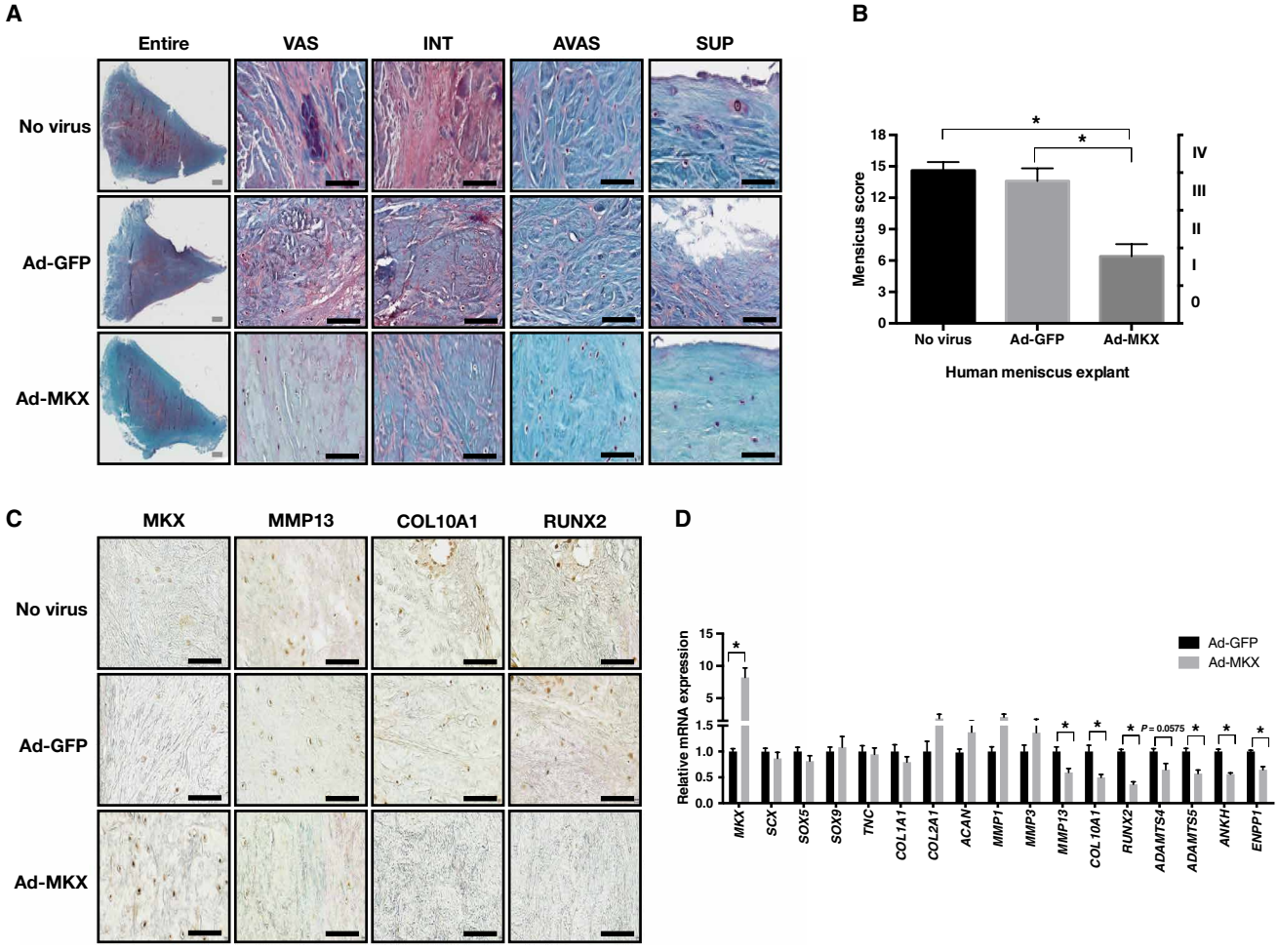

Fig. 7. Ad-MKX injection into human meniscus explants from patients with OA. Ad-GFP or Ad-MKX virus (1×10^{10} pfu/ml) was injected into OA meniscus explants ($n = 6$; female, age 68 to 74; mean, 71 ± 2). Explants were cultured for 2 weeks until analysis. (**A**) Safranin-O staining of the human meniscus explants showing the entire meniscus, vascular (VAS), intermediate (INT), avascular (AVA), and superficial area (SUP). (**B**) Meniscus histopathological scores. *$P < 0.05$ (one-way ANOVA) compared to the selected group. (**C**) Immunohistochemistry for MKX, MMP13, COL10A1, and RUNX2. (**D**) qRT-PCR analysis of genes related to meniscus ECM, degeneration, hypertrophy, inflammation, and calcification. *$P < 0.05$ (Mann-Whitney test) compared to the Ad-GFP–injected meniscus group. All values are means ± SEM. Gray scale bars, 1 mm; black scale bars, 100 μm.

which TFs are expressed and enriched in meniscus, we performed RNA-seq on human meniscus and used RNA-seq data on 37 other tissues in the GTEx database. This identified 55 TFs that are enriched in meniscus when comparing RNA-seq from meniscus with GTEx without cartilage and 14 TFs when comparing meniscus with GTEx including cartilage. MKX was the second most ME TF, after *ZNF573*. To overcome the limitation that there were no RNA-seq data of tendon/ligaments in the GTEx dataset, we confirmed by additional PCR analyses that MKX is expressed higher in meniscus than in cartilage and undifferentiated MSC and at similar expression as in ligaments. MKX expression showed zonal differences between vascular and avascular meniscus although MKX was highly expressed throughout the entire meniscus. Cell populations in the vascular zone are more fibroblastic, whereas the cells in the avascular zone have a more chondrocytic phenotype (*26*). MKX expression was higher in the former, consistent with its antagonism to chondrocytic differentiation of MSCs (*27*). MKX is a member of the Iroquois (Irx) gene family, and its expression in meniscus was higher than that of all other Irx genes. These findings suggested that MKX is an enriched TF in meniscus and is associated with differentiation or maintenance of meniscus cells.

Studies on the role of MKX in MSC differentiation to the meniscus cell phenotype showed that Ad-MKX promoted fibrogenic differentiation. To induce expression of chondrogenic markers in MKX-transduced MSCs, we added TGF-β3 (*11*). Some meniscus ECM proteins such as COL1A1 and ACAN were increased, but COL2A1 was not increased. However, the combination of MKX and TGF-β3 increased meniscus-specific ECM proteins, most closely resembling normal meniscus cells. During in vitro chondrogenesis of MSC, COL2A1 expression precedes COL10A1 and other markers of hypertrophy (*28*). TGF-β induces chondrogenesis in MSCs including markers of the hypertrophic phenotype (*29*). MKX decreased *COL10A1*, *RUNX2*, and *MMP13* expression and increased *COL1A1* in the MSC pellets. Ad-MKX and TGF-β3 synergistically increased *SCX*, *COL2A1*, *ACAN*, *CHAD*, *COMP*, *DCN*, and *MMP13*. However, in this combination with TGF-β3, Ad-MKX decreased not only

COL10A1 but also *RUNX2*. In the present study, Ad-MKX–transduced MSCs alone promoted meniscal phenotype without hypertrophy. Moreover, *COMP*, a marker of meniscus cells (*30*), was highly increased after Ad-MKX and TGF-β3 treatment. *COMP* is an early indicator of chondrogenesis in MSCs, and it is induced by the TGF-β signaling pathway and by *SOX5*, *SOX6*, and *SOX9* (*31*). In this study, *COMP* was increased by TGF-β3, although MKX suppressed *SOX* TFs. Prior studies to generate meniscus cells from MSCs used growth factors, including TGF-β1 (*19*) and sequential treatment with CTGF and TGF-β3 (*11*). The expression patterns of *COL1A1*, *COL2A1*, and *ACAN* appear to be similar to those in the present study, but hypertrophy markers and other TFs were not analyzed in the prior studies.

Overall, these results indicate that the combination of MKX and TGF-β3 induces MSC differentiation to a phenotype that very closely resembles meniscus cells with a marker profile that includes *COL1A1*, *COL2A1*, *ACAN*, *CHAD*, *COMP*, and *DCN*. Mechanisms by which MKX regulates differentiation include its effects on other TFs, including *SOX5*, *SOX9*, *SCX*, and *RUNX2*.

Our studies also examined the role of MKX in regulating gene expression in mature human meniscus cells. In cells from normal human meniscus, MKX suppressed the expression of genes related to meniscus degeneration and calcification. MKX also regulated other TFs: It suppressed *SOX5* and *RUNX2* and increased *SCX* in cells from human meniscus. MKX knockdown in meniscus cells up-regulated TFs such as *SOX5*, *SCX*, and *RUNX2*; hypertrophic chondrocyte markers *MMP13* and *RUNX2*; and *ENPP1*, which has been linked with meniscus calcification in aging and OA (*32*, *33*). In cells from human OA menisci, MKX suppressed the abnormal basal expression of these pathogenesis-related genes and it also antagonized the IL-1β–mediated up-regulation in normal and OA meniscus cells. Thus, the effect of MKX on differentiation is cell type and context dependent. In MSCs, Ad-MKX alone induces a tenocyte-like phenotype as reported (*27*). The addition of TGF-β3 to Ad-MKX induces a phenotype similar to meniscus cells. In mature normal meniscus cells, Ad-MKX alone stabilizes this phenotype and corrects some of the abnormally expressed genes in OA meniscus cells.

Next, we explored the therapeutic potential of MKX for the healing of meniscus tears by using adenoviral gene transfer (*34*, *35*). This approach has the advantage of introducing cells and a therapeutic gene product to the injured site. For the first trial of ex vivo gene delivery of a meniscus-associated TF, we used an experimentally induced tear in the avascular region of bovine meniscus, a previously validated model (*19*–*21*). We selected DMS as a tissue-derived material because it provides a natural environment for cell seeding, migration, and ECM deposition (*36*) and because it is suitable for TGF-β3 immobilization. The DMS allowed MSC attachment and, when conjugated with heparin and TGF-β3, increased MSC proliferation. We then compared DMS alone to combinations of MSCs with or without MKX and DMS with or without TGF-β3. Among the various groups tested, comparison of MSC-DMS with DMS alone only showed marginal effects on interconnectivity. The maximum efficacy was dependent on TGF-β3 conjugation with MSCs on DMS. The combination of Ad-MKX–transduced MSCs and TGF-β3–conjugated DMS resulted in the highest cell proliferation, glycosaminoglycan staining, cell infiltration into the DMS, and collagen fiber interconnectivity, suggesting that there is a synergistic effect of Ad-MKX overexpression and TGF-β3 for cell proliferation and de novo glycosaminoglycan synthesis. A previous study indicated that migratory meniscus progenitor cells are controlled through the TGF-β pathway (*37*), and it is possible that a similar subset of cells was recruited to the DMS/meniscus interface in the present study.

To test the in vivo efficacy of MKX, we used the DMM model in which surgical DMM leads to progressive meniscus damage and OA-like changes in articular cartilage (*22*). Intra-articular Ad-GFP injection led to infection of meniscus and other joint tissues such as synovium and articular cartilage. There was no detection of any synovial hyperplasia or leukocyte infiltration. We found infiltrated cells from synovium expressing MKX on the outer surface of meniscus and inside the damaged meniscus in joints that had been subjected to DMM. However, MKX expression in Ad-GFP–injected sham group was weaker than in Ad-MKX–injected sham group. Moreover, MKX expression in Ad-MKX–injected DMM group was stronger than in Ad-GFP–injected sham group. Intra-articular Ad-MKX injection decreased the severity of the histological changes in meniscus, articular cartilage, and synovium. Ad-MKX also suppressed *COL10A1* and *RUNX2* in mouse meniscus and cartilage, consistent with the in vitro observations.

In an ex vivo model with human OA meniscus explants, Ad-MKX injection improved histopathology and reduced the expression of markers related to hypertrophic differentiation, inflammation, and calcification. These results suggest that MKX gene transfer or small molecules that induced MKX may be useful in correcting the abnormal gene expression patterns in OA meniscus.

The present results suggest a potential therapeutic benefit of MKX; however, additional in vivo experiments are needed to demonstrate that MKX-transduced MSCs can heal meniscus defects in vivo. The efficacy of virus-mediated MKX gene transfer into joints with injured menisci needs to be further examined in larger animals and at later time points after injury. Whether MKX can be used to prevent further degradation of aging-related meniscus damage and associated OA requires analysis in appropriate animal models.

In conclusion, we show that MKX is a TF that is highly expressed and enriched in meniscus and that it regulates the expression of other TFs (*SOX5*, *SOX9*, *SCX*, and *RUNX2*) and the phenotype of cells from avascular and vascular meniscus. Our results also indicate that Ad-MKX in combination with TGF-β3 is effective in promoting differentiation of MSCs toward a meniscus cell phenotype. Seeding MKX-transduced MSCs on heparin/TGF-β3–conjugated DMS is a useful construct for meniscus tissue engineering, repair, and regeneration. Approaches to deliver MKX to joints with meniscus injury have potential to protect against meniscus degeneration and OA development.

MATERIALS AND METHODS

Study design

The goal of the study was to identify which TFs are enriched, govern meniscus cell phenotype and tissue repair, and affect OA progression. To allow a genome-wide analysis, we generated RNA-seq data from human knee menisci and articular cartilage and compared them with RNA-seq data in the GTEx database. This identified MKX as one of the most highly enriched TFs in meniscus. To confirm these results, qPCR analysis was performed on additional meniscus and cartilage samples, ACL, and MSCs. To determine whether MKX expression is altered in disease, we analyzed its expression in menisci from normal and OA-affected menisci. The potential role of MKX in inducing meniscus cell differentiation of MSCs was analyzed by adenoviral transduction (Ad-MKX) of these cells and culturing them

in the presence of several growth factors. The function of MKX in human meniscus cells was also examined by infection of the cells with Ad-MKX or transfection with MKX siRNA and analyzing genes related to meniscus ECM and cell differentiation. The potential of MKX to suppress disease-related genes was tested by culturing Ad-MKX–infected meniscus cells with proinflammatory cytokine IL-1β. We used meniscus tissue explants with experimental meniscus tears to evaluate meniscus healing by inserting a scaffold that was conjugated with TGF-β3 and seeded with Ad-MKX–infected MSCs. The explants were examined by histology and for mechanical properties. A mouse model of meniscus injury was used as an in vivo model to test whether intra-articular injections of Ad-MKX promoted meniscus healing and protected against OA. Meniscus explants from patients with OA undergoing knee replacement surgery were infected with Ad-MKX to determine whether MKX can reduce expression of genes that promote OA-associated meniscus degradation.

Human subjects

All human tissues were obtained with approval by the Scripps Human Subjects Committee. Intact knee joints were procured by tissue banks from 20 donors aged 37.5 ± 9.75 years (range, 18 to 57) and processed within 24 to 48 hours postmortem. The donors had no history of joint disease, and upon macroscopic inspection, all cartilage and meniscus surfaces were intact. Full-thickness cartilage was harvested for RNA isolation from identical locations on the medial and lateral femoral condyles. Meniscus tissue was harvested from vascular and avascular regions.

GTEx RNA-seq data

We used RNA-seq data generated by GTEx project (*12*, *13*). We included 37 human tissues from GTEx with expression data for at least 3 samples and a maximum of 25 samples from unique subjects with age less than 50 years. The cartilage RNA-seq data was from 15 normal human knee cartilage as previously described (*38*) and 10 normal meniscus samples (vascular and avascular meniscus samples from the same donors) and meniscus RNA-seq data (described below), resulting in a total of 729 samples and 39 tissues that were included in the present analysis. The aligned RNA-seq datasets were unstranded and ranged from 30 million to 200 million paired-end reads each.

Tissue processing, RNA, and DNA isolation

Meniscus tissue was resuspended in RNAlater and cartilage in Allprotect Tissue Reagent (QIAGEN) immediately after harvest. For RNA isolation, meniscus and cartilage tissues were pulverized using a 6770 Freezer/Mill cryogenic grinder (SPEX SamplePrep) and homogenized in QIAzol Lysis Reagent (QIAGEN). RNA was extracted from meniscus using a fibrous tissue RNA extraction kit (QIAGEN). For cartilage samples, RNA was isolated using an RNAqueous kit (Ambion). After isolation, on-column DNase (deoxyribonuclease) treatment was performed using the DNase I (QIAGEN) and the RNeasy MinElute Cleanup Kit (QIAGEN). RNA purity was assessed using NanoDrop (ND-1000, Thermo Fisher Scientific) and quantified by Qubit 2.0 Fluorometer, using the RNA Assay Kit (Invitrogen). Sample quality was determined with the Agilent 2100 Bioanalyzer using the RNA 6000 Nano LabChip (Agilent, 5067-1511).

RNA sequencing

RNA samples were sequenced using 125 to 150 ng of total RNA as input. Sequencing mRNA libraries were prepared using the Encore Complete RNA-Seq DR Multiplex System 1-8 and 9-16 (NuGEN). RNA libraries were prepared using an Illumina TruSeq small RNA sample prep kit. Samples of each batch were pooled at equal amount of cDNA before sequencing to control for lane and batch effects. Two lanes of an Illumina HiSeq 2000 instrument were used to generate a total of 8 million to 30 million 100–base pair reads.

The Illumina Genome Analyzer Pipeline Software (CASAVA version 1.8.2) was used to convert the original image data generated by the sequencing machine into sequence data via base calling to generate fastq files and to demultiplex the samples. We performed a per base sequence quality check using the software FastQC (version 0.10.1; www.bioinformatics.babraham.ac.uk/projects/fastqc/) before read mapping. The number of reads sequenced ranged from 15 million to 26 million reads per sample, with greater than 60% of these reads aligning to the human genome (hg19).

Gene expression and normalization

The raw RNA-seq FASTA files were processed using the count-based differential expression analysis best practice protocol (*39*) to quantify for gene expression. Accordingly, sequencing reads were aligned to the human genome (hg19) using the STAR aligner (*40*). HTSeq was used to count the number of reads unambiguously overlapping each gene, where each gene was considered to be the union of its exons (*39*) with UCSC RefSeq hg19 annotation (release 57). Sample normalization factors were computed using the edgeR TMM method (*41*). Only genes with average gene expression above $\log_2$CPM of 3.0 in at least 1 of the 39 tissues were considered expressed and used in subsequent analyses, resulting in a gene list of 17,333 informative genes. We converted the gene symbols to Entrez IDs using mygene (*42*). Of the 17,333 genes, 881 gene symbols did not have an associated Entrez ID and were discarded from this study. The resulting genes with Entrez IDs correspond to the set of "background or detected genes" consisting of 16,452 genes. The distribution (by $\log_2$CPM) of genes expressed in meniscus was similar to the other 38 tissues analyzed (fig. S14).

Identification of meniscus-expressed and ME genes

To compare the number of genes expressed in each tissue, we used several $\log_2$CPM cutoffs and found that each threshold resulted in similar results with testis having the highest number of expressed genes and blood having the lowest, followed by meniscus (fig. S15). For our subsequent analyses, we used a $\log_2$CPM > 3 cutoff to reduce variability due to genes expressed at very low counts. Using this cutoff, we identified 9730 genes that were expressed in meniscus.

For identifying ME genes, raw counts of the 16,452 filtered "background genes" were transformed to $\log_2$CPM and then quantile-normalized, and observation weights were computed using the Voom method (*43*). To identify genes whose expression was higher in meniscus than every other tissue, we first excluded all genes for which meniscus was not the highest-expressed tissue. We then identified the tissue with the second-highest average expression (lowest fold change), and ME genes were defined as those having a $P < 0.01$ and a $\log_2$FC > 1 relative to that tissue.

TFs among the ME genes

To identify TFs among ME genes, we searched which of the 313 ME genes were among the 1209 genes classified under GO term TF activity, sequence-specific DNA binding (GO, 0003700) (*14*).

Meniscus explants, meniscus cells, and MSCs

Normal bovine menisci were obtained from fresh bovine knees (Animal Technologies Inc.). To prepare meniscus explants, the avascular region was resected with a scalpel and cut into blocks of about 20-mm width. Cylindrical explants, 12 mm in diameter, were harvested from the blocks by using a specimen needle and precultured for 2 to 3 days at 37°C, 5% CO_2 until starting the experiment. Human BM-MSCs from 21- to 23-year-old donors were purchased from Lonza (Walkersville, MD) and cultured in Lonza MSCGM human Mesenchymal Stem Cell Growth BulletKit Medium (basal media for BM-MSCs).

Human meniscus and synovium were harvested from normal human knee joints. Vascular meniscus, avascular meniscus, and synovium were minced and digested separately with 2% collagenase for 12 hours. SYN-MSCs and meniscus cells were cultured in Dulbecco's modified Eagle's medium (DMEM) with 10% calf serum (CS) and 1% penicillin-streptomycin-glutamine (PSG) (basal media for meniscus cells and SYN-MSCs).

Validation of tissue-specific gene expression by quantitative reverse transcription PCR

Intact normal human knee joints were obtained from tissue banks. Cartilage (n = 5), meniscus (n = 7), and ACL (n = 8) were stored at −20°C in Allprotect Tissue Reagent (QIAGEN). Tissues were pulverized using a 6770 Freezer/Mill cryogenic grinder (SPEX SamplePrep); human BM-MSCs (n = 8) from monolayer culture were collected, and RNA was isolated, purified, and quantified as previously described (*44*). qPCR analysis was conducted on a LightCycler 480 Real-Time PCR System (Roche Diagnostics) using TaqMan Gene Expression Assay probes (Life Technologies; table S3). The mRNA expression values were calculated as relative quantities in comparison to GAPDH (glyceraldehyde phosphate dehydrogenase).

Adenoviral vector construction

The plasmid pCR Blunt-MKX/myc was digested with Eco RV and Spe I. Then, the myc-tagged MKX gene fragment was cloned into the plasmid pENTR1A MCS to construct the recombinant pENTR1A-MKX/myc plasmid. Both recombinant pAd/CMV/V5-DEST vector plasmids expressing GFP and MKX were linearized with Pac I, followed by transfection of human embryonic kidney–293A cells using Lipofectamine 2000 (Life Technologies). The sequential steps of adenovirus recovery, large-scale viral production, concentration, purification, and titration were performed as described (*45*–*47*). Ad-GFP [8×10^9 plaque-forming units (pfu)/ml] and Ad-MKX (4×10^8 to 2×10^{10} pfu/ml) viral particles were aliquoted, stored at −80°C, and used to transduce MSCs.

Adenoviral transduction of MSCs

For viral infection, dilutions of Ad-GFP and Ad-MKX stocks in MSCGM for BM-MSCs or DMEM with 1% CS and 1% PSG for SYN-MSCs as viral infection medium were applied to the cells. After 6-hour incubation at 37°C, the viral infection medium was removed, and the infected cells were washed with phosphate-buffered saline (PBS) and further incubated in basal media for 48 hours.

Cell viability

The viability of the MSCs was determined by thiazolyl blue tetrazolium bromide, 4,5-dimethylthiazol-2-yl-2,5-diphenyltetrazolium bromide. The amount of 25 μl was added to the cells and incubated for 5 hours without light. The media were aspirated, and 100 μl of dimethyl sulfoxide was added and mixed. The plates were read at 540 nm on a microplate reader. The triplicate data were normalized by respective controls.

MSC chondrogenesis culture

Cells were spun at 800 rpm for 5 min to prepare pellets and then incubated in 15-ml conical tubes with loosened caps. The chondrogenic induction supplements were mixed with insulin, transferrin, sodium selenite (ITS), with sodium pyruvate (11 mg/ml) (1×; Invitrogen, Carlsbad, CA), 0.1 μM dexamethasone, L-ascorbic acid 2-phosphate (50 μg/ml), and L-proline (40 μg/ml).

Adenoviral overexpression and siRNA knockdown of MKX in meniscus cells

For adenoviral infection, Ad-MKX (2×10^{10} pfu/ml) or Ad-GFP (1×10^{10} pfu/ml) control virus at MOI of 100 in DMEM with 1% CS and 1% PSG was applied to the cells. For siRNA transfection, the mixture of 3 μl of Lipofectamine RNAiMAX reagent (13778-150, Thermo Fisher Scientific) and 1 μl of MKX siRNA (0.5 nmol; s49085, Thermo Fisher Scientific) in 100 μl of DMEM without CS and PSG was applied to the cells. After 6-hour incubation at 37°C, adenoviral infection media were discarded, and the cells were washed with PBS and incubated in basal media for 48 hours.

Adenoviral overexpression of MKX in IL-1β–treated meniscus cells

Meniscus cells were transduced by Ad-MKX or Ad-GFP as mentioned above. After 48 hours, IL-1β (0.5 ng/ml) was added, and cells were cultured for additional 72 hours. RNA was isolated for qRT-PCR (quantitative reverse transcription PCR) analysis.

Preparation of DMS and growth factor conjugation

Explants were obtained from bovine meniscus using specimen needles and decellularized as described (*48*, *49*). Heparin was conjugated to the DMS to immobilize TGF-β3 (*50*). The heparin-DMS were rinsed three times with distilled water and incubated with TGF-β3 (200 ng/ml; PeproTech Inc.) for 12 hours at 4°C. DMS were washed with PBS three times and stored at 4°C.

DMS preculture and ex vivo meniscus explant culture

MSCs were seeded at 5×10^5 per 6-mm-diameter DMS and preincubated in basal media with or without chondrogenic induction supplements, including TGF-β3 (10 ng/ml, w/v), ITS-X (1× volume), L-ascorbic acid 2-phosphate (50 μg/ml, w/v), L-proline (40 μg/ml, w/v), dexamethasone (0.1 μM), and sodium pyruvate (100 μg/ml, w/v) for 3 days. In 12-mm-diameter bovine meniscus explants, full-thickness radial tears were created in the middle segment of the explant using a blade. DMS were inserted into defect. The explants were cultured for 2 and 4 weeks with medium change every 3 days.

Histological and immunohistochemical analyses

The meniscus explants were fixed in Z-Fix (Anatech). Paraffin-embedded sections (5 to 7 μm) were stained with Safranin-O to detect glycosaminoglycan. Fast green was used as a counterstain. The following antibodies were used: MKX (1:200; HPA006927, Sigma-Aldrich), COL1A1 (1:200; AB292, Abcam), COL2A1 [1:50; II-II6B3-S, DSHB (Developmental Studies Hybridoma Bank)], ACAN (1:50; L0101, Assay Biotechnology), MMP13 (1:600; AB39012, Abcam),

COL10A1 (1:10; X-AC9, DSHB), and RUNX2 (1:75; SC-390351, Santa Cruz Biotechnology). Mouse IgG (immunoglobulin G) (I-2000, Vector Laboratories Inc.) or rabbit IgG (I-1000, Vector Laboratories Inc.) were used as negative controls (fig. S16). There was only weak staining for COL1A1 and COL2A1 in DMS compared with bovine meniscus explants (fig. S17). For quantitative analysis of DAPI (H-1500, Vector Laboratories Inc.) staining, the cells in the DMS and at the borderline between DMS in injured explants were counted. Polarized picrosirius red staining and DIC microscopy were used to detect collagen types and fiber alignment within the explants and to examine the fibrous interconnectivity between inserted DMS and injured explants. Histopathological scoring of meniscus, articular cartilage, and synovium was performed by previous methods (*51*–*54*).

Biomechanical testing

The tensile stiffness of the injured meniscus explants cultured with various types of DMS was quantified by tensile testing (n = 8 to 12 per group). Explants were fixed vertically at both ends in the grips of a uniaxial testing machine (Instron Universal Testing Machine, 3342 Single Column Model) with a 500-N load cell and tested to failure at a crosshead speed of 1 mm/min at a gauge length of 20 mm under ambient conditions. Tensile stiffness was calculated from the slope of the linear segment of the stress-strain curve.

DMM model in mice

All animal studies were performed with approval by the Scripps Institutional Animal Care and Use Committee. BALB/cByJ mice [12 weeks of age; males (n = 5), 27.4 ± 1.4 g; females (n = 6), 22.9 ± 1.5 g] were used. Surgical approach was to the right mouse knee joint with a medial parapatellar ligament incision (*22*). Fat pad was dissected, and medial meniscus and medial meniscotibial ligament (MMTL) were identified. The MMTL was transected using microscissors, and the meniscus was confirmed to be free to displace medially. After the surgical procedure, the joint capsule and skin were sequentially closed with dermal glue, and at 1 week after surgery, 10 μl (1×10^{10} pfu/ml) of Ad-GFP or Ad-MKX virus was injected into mouse knee joints once per week for 4 weeks.

Ad-MKX infection of human meniscus explants

Human menisci were collected from patients with OA undergoing joint replacement surgery (n = 6; female, age 68 to 74; mean, 71 ± 2). From each meniscus, a 5-mm-thick block including avascular and vascular regions was resected from the central region, or body was resected and cut into three pieces, and one each was used for control, Ad-GFP injection, or Ad-MKX injection. The explants were washed three times in DMEM with 1% antibiotic-antimycotic media. A 1-ml syringe with a 31-gauge needle containing Ad-GFP or Ad-MKX virus (1×10^{10} pfu/ml, 20 μl) was used to inject 10 μl into the superior and 10 μl into the inferior side of meniscus. The explants were cultured in basal media for 2 weeks. Half of each explant was used for qRT-PCR, and half was used for histology.

Statistical analyses

Data represent means and SEM, from at least three to four replicate studies. Results were analyzed using Prism version 7 (GraphPad Software Inc.). Fold change in gene expression was calculated using the ddCt method based on the average of technical duplicates. All samples were normalized to the average delta Ct of negative controls. Statistical significance was determined using a Mann-Whitney test between two groups, and one-way analysis of variance (ANOVA) was used to compare multiple groups. Results with $P < 0.05$ (95% confidence interval) were considered statistically significant. Subject-level data are reported in data file S1.

SUPPLEMENTARY MATERIALS

stm.sciencemag.org/cgi/content/full/12/567/eaan7967/DC1

Fig. S1. ME TFs compared with GTEx tissues and articular cartilage.
Fig. S2. Evaluation of MKX expression between human cartilage zones.
Fig. S3. Viability assay and gene expression in human BM-MSCs transduced with Ad-MKX and microscopy of Ad-GFP–transduced BM-MSCs.
Fig. S4. mRNA expression in Ad-MKX–transduced human SYN-MSCs after 10-day monolayer culture.
Fig. S5. Comparative analysis of RNA-seq count values between human meniscus and cartilage.
Fig. S6. qRT-PCR analysis of Ad-MKX–transduced human vascular and avascular cells.
Fig. S7. Decellularization, heparin, and TGF-β3 conjugation of bovine meniscus tissue.
Fig. S8. Cellularity of MSC-seeded DMS.
Fig. S9. Histology and GFP fluorescence of mouse knee joints.
Fig. S10. Safranin-O staining and immunohistochemistry of Ad-GFP– or Ad-MKX–injected mouse knee joints after DMM surgery.
Fig. S11. Safranin-O staining of Ad-GFP– or Ad-MKX–injected mouse knee joints after DMM surgery.
Fig. S12. Immunohistochemistry of Ad-GFP– or Ad-MKX–injected mouse knee joints after DMM surgery.
Fig. S13. Immunohistochemistry and histology of Ad-GFP– or Ad-MKX–injected human meniscus explants from patients with OA.
Fig. S14. Density plot of $\log_2$CPM expression values for all tissues.
Fig. S15. Gene expression in tissues above thresholds.
Fig. S16. Negative controls for immunohistochemistry.
Fig. S17. Immunohistochemistry of DMS in bovine meniscus explant.
Table S1. ME TFs compared with GTEx tissues.
Table S2. ME TFs compared with GTEx tissue and articular cartilage.
Table S3. TaqMan qRT-PCR probe information.
Data file S1. Subject-level data.

View/request a protocol for this paper from *Bio-protocol*.

REFERENCES AND NOTES

1. C. Laible, D. A. Stein, D. N. Kiridly, Meniscal repair. *J. Am. Acad. Orthop. Surg.* **21**, 204–213 (2013).
2. K. E. DeHaven, Meniscus repair. *Am. J. Sports Med.* **27**, 242–250 (1999).
3. G. C. Keene, D. Bickerstaff, P. J. Rae, R. S. Paterson, The natural history of meniscal tears in anterior cruciate ligament insufficiency. *Am. J. Sports Med.* **21**, 672–679 (2016).
4. M. Cipolla, A. Scala, E. Gianni, G. Puddu, Different patterns of meniscal tears in acute anterior cruciate ligament (ACL) ruptures and in chronic ACL-deficient knees. *Knee Surg. Sports Traumatol. Arthrosc.* **3**, 130–134 (1995).
5. M. J. Feucht, S. Bigdon, G. Bode, G. M. Salzmann, D. Dovi-Akue, N. P. Sudkamp, P. Niemeyer, Associated tears of the lateral meniscus in anterior cruciate ligament injuries: Risk factors for different tear patterns. *J. Orthop. Surg. Res.* **10**, 34 (2015).
6. F. W. Roemer, C. K. Kwoh, M. J. Hannon, D. J. Hunter, F. Eckstein, T. Fujii, R. M. Boudreau, A. Guermazi, What comes first? Multitissue involvement leading to radiographic osteoarthritis: Magnetic resonance imaging-based trajectory analysis over four years in the osteoarthritis initiative. *Arthritis Rheumatol.* **67**, 2085–2096 (2015).
7. B. E. Oiestad, L. Engebretsen, K. Storheim, M. A. Risberg, Knee osteoarthritis after anterior cruciate ligament injury: A systematic review. *Am. J. Sports Med.* **37**, 1434–1443 (2009).
8. S. M. Imler, A. N. Doshi, M. E. Levenston, Combined effects of growth factors and static mechanical compression on meniscus explant biosynthesis. *Osteoarthr. Cartil.* **12**, 736–744 (2004).
9. L. C. Ionescu, G. C. Lee, K. L. Huang, R. L. Mauck, Growth factor supplementation improves native and engineered meniscus repair in vitro. *Acta Biomater.* **8**, 3687–3694 (2012).
10. C. H. Lee, B. Shah, E. K. Moioli, J. J. Mao, CTGF directs fibroblast differentiation from human mesenchymal stem/stromal cells and defines connective tissue healing in a rodent injury model. *J. Clin. Invest.* **120**, 3340–3349 (2010).
11. C. H. Lee, S. A. Rodeo, L. A. Fortier, C. Lu, C. Erisken, J. J. Mao, Protein-releasing polymeric scaffolds induce fibrochondrocytic differentiation of endogenous cells for knee meniscus regeneration in sheep. *Sci. Transl. Med.* **6**, 266ra171 (2014).
12. GTEx Consortium, The Genotype-Tissue Expression (GTEx) project. *Nat. Genet.* **45**, 580–585 (2013).
13. GTEx Consortium, The Genotype-Tissue Expression (GTEx) pilot analysis: Multitissue gene regulation in humans. *Science* **348**, 648–660 (2015).

14. A. Alexa, J. Rahnenfuhrer, T. Lengauer, Improved scoring of functional groups from gene expression data by decorrelating GO graph structure. *Bioinformatics* **22**, 1600–1607 (2006).
15. A. Lomniczi, H. Wright, J. M. Castellano, V. Matagne, C. A. Toro, S. Ramaswamy, T. M. Plant, S. R. Ojeda, Epigenetic regulation of puberty via Zinc finger protein-mediated transcriptional repression. *Nat. Commun.* **6**, 10195 (2015).
16. S. P. Grogan, S. F. Duffy, C. Pauli, J. A. Koziol, A. I. Su, D. D. D'Lima, M. K. Lotz, Zone-specific gene expression patterns in articular cartilage. *Arthritis Rheum.* **65**, 418–428 (2013).
17. B. O. Diekman, C. R. Rowland, D. P. Lennon, A. I. Caplan, F. Guilak, Chondrogenesis of adult stem cells from adipose tissue and bone marrow: Induction by growth factors and cartilage-derived matrix. *Tissue Eng. Part A* **16**, 523–533 (2010).
18. K. I. Lee, M. Olmer, J. Baek, D. D. D'Lima, M. K. Lotz, Platelet-derived growth factor-coated decellularized meniscus scaffold for integrative healing of meniscus tears. *Acta Biomater.* **76**, 126–134 (2018).
19. A. F. Steinert, G. D. Palmer, R. Capito, J. G. Hofstaetter, C. Pilapil, S. C. Ghivizzani, M. Spector, C. H. Evans, Genetically enhanced engineering of meniscus tissue using ex vivo delivery of transforming growth factor-β1 complementary deoxyribonucleic acid. *Tissue Eng.* **13**, 2227–2237 (2007).
20. K. Shimomura, B. B. Rothrauff, R. S. Tuan, Region-specific effect of the decellularized meniscus extracellular matrix on mesenchymal stem cell-based meniscus tissue engineering. *Am. J. Sports Med.* **45**, 604–611 (2017).
21. J. Baek, S. Sovani, N. E. Glembotski, J. Du, S. Jin, S. P. Grogan, D. D. D'Lima, Repair of avascular meniscus tears with electrospun collagen scaffolds seeded with human cells. *Tissue Eng. Part A* **22**, 436–448 (2016).
22. S. S. Glasson, T. J. Blanchet, E. A. Morris, The surgical destabilization of the medial meniscus (DMM) model of osteoarthritis in the 129/SvEv mouse. *Osteoarthr. Cartil.* **15**, 1061–1069 (2007).
23. S. Bhattacharyya, S. J. Chen, M. Wu, M. Warner-Blankenship, H. Ning, G. Lakos, Y. Mori, E. Chang, C. Nihijima, K. Takehara, C. Feghali-Bostwick, J. Varga, Smad-independent transforming growth factor-beta regulation of early growth response-1 and sustained expression in fibrosis: Implications for scleroderma. *Am. J. Pathol.* **173**, 1085–1099 (2008).
24. D. E. Pazin, L. W. Gamer, L. P. Capelo, K. A. Cox, V. Rosen, Gene signature of the embryonic meniscus. *J. Orthop. Res.* **32**, 46–53 (2014).
25. V. Lejard, F. Blais, M. J. Guerquin, A. Bonnet, M. A. Bonnin, E. Havis, M. Malbouyres, C. B. Bidaud, G. Maro, P. Gilardi-Hebenstreit, J. Rossert, F. Ruggiero, D. Duprez, EGR1 and EGR2 involvement in vertebrate tendon differentiation. *J. Biol. Chem.* **286**, 5855–5867 (2011).
26. S. P. Grogan, C. Pauli, M. K. Lotz, D. D. D'Lima, Relevance of meniscal cell regional phenotype to tissue engineering. *Connect. Tissue Res.* **58**, 259–270 (2017).
27. K. Otabe, H. Nakahara, A. Hasegawa, T. Matsukawa, F. Ayabe, N. Onizuka, M. Inui, S. Takada, Y. Ito, I. Sekiya, T. Muneta, M. Lotz, H. Asahara, Transcription factor Mohawk controls tenogenic differentiation of bone marrow mesenchymal stem cells in vitro and in vivo. *J. Orthop. Res.* **33**, 1–8 (2015).
28. K. Pelttari, A. Winter, E. Steck, K. Goetzke, T. Hennig, B. G. Ochs, T. Aigner, W. Richter, Premature induction of hypertrophy during in vitro chondrogenesis of human mesenchymal stem cells correlates with calcification and vascular invasion after ectopic transplantation in SCID mice. *Arthritis Rheum.* **54**, 3254–3266 (2006).
29. M. B. Mueller, M. Fischer, J. Zellner, A. Berner, T. Dienstknecht, L. Prantl, R. Kujat, M. Nerlich, R. S. Tuan, P. Angele, Hypertrophy in mesenchymal stem cell chondrogenesis: Effect of TGF-beta isoforms and chondrogenic conditioning. *Cells Tissues Organs* **192**, 158–166 (2010).
30. G. Müller, A. Michel, E. Altenburg, COMP (cartilage oligomeric matrix protein) is synthesized in ligament, tendon, meniscus, and articular cartilage. *Connect. Tissue Res.* **39**, 233–244 (1998).
31. H. Li, D. R. Haudenschild, K. L. Posey, J. T. Hecht, P. E. Di Cesare, J. H. Yik, Comparative analysis with collagen type II distinguishes cartilage oligomeric matrix protein as a primary TGFβ-responsive gene. *Osteoarthr. Cartil.* **19**, 1246–1253 (2011).
32. Y. Sun, D. R. Mauerhan, Meniscal calcification, pathogenesis and implications. *Curr. Opin. Rheumatol.* **24**, 152–157 (2012).
33. M. F. Rai, D. Patra, L. J. Sandell, R. H. Brophy, Transcriptome analysis of injured human meniscus reveals a distinct phenotype of meniscus degeneration with aging. *Arthritis Rheum.* **65**, 2090–2101 (2013).
34. C. Evans, Using genes to facilitate the endogenous repair and regeneration of orthopaedic tissues. *Int. Orthop.* **38**, 1761–1769 (2014).
35. C. H. Evans, P. D. Robbins, Genetically augmented tissue engineering of the musculoskeletal system. *Clin. Orthop. Relat. Res.* , S410–S418 (1999).
36. E. A. Makris, P. Hadidi, K. A. Athanasiou, The knee meniscus: Structure-function, pathophysiology, current repair techniques, and prospects for regeneration. *Biomaterials* **32**, 7411–7431 (2011).
37. H. Muhammad, B. Schminke, C. Bode, M. Roth, J. Albert, S. von der Heyde, V. Rosen, N. Miosge, Human migratory meniscus progenitor cells are controlled via the TGF-β pathway. *Stem Cell Rep.* **3**, 789–803 (2014).
38. K. M. Fisch, R. Gamini, O. Alvarez-Garcia, R. Akagi, M. Saito, Y. Muramatsu, T. Sasho, J. A. Koziol, A. I. Su, M. K. Lotz, Identification of transcription factors responsible for dysregulated networks in human osteoarthritis cartilage by global gene expression analysis. *Osteoarthr. Cartil.* **26**, 1531–1538 (2018).
39. S. Anders, P. T. Pyl, W. Huber, HTSeq—A Python framework to work with high-throughput sequencing data. *Bioinformatics* **31**, 166–169 (2015).
40. A. Dobin, C. A. Davis, F. Schlesinger, J. Drenkow, C. Zaleski, S. Jha, P. Batut, M. Chaisson, T. R. Gingeras, STAR: Ultrafast universal RNA-seq aligner. *Bioinformatics* **29**, 15–21 (2013).
41. M. D. Robinson, D. J. McCarthy, G. K. Smyth, edgeR: A bioconductor package for differential expression analysis of digital gene expression data. *Bioinformatics* **26**, 139–140 (2010).
42. J. Xin, A. Mark, C. Afrasiabi, G. Tsueng, M. Juchler, N. Gopal, G. S. Stupp, T. E. Putman, B. J. Ainscough, O. L. Griffith, A. Torkamani, P. L. Whetzel, C. J. Mungall, S. D. Mooney, A. I. Su, C. Wu, High-performance web services for querying gene and variant annotation. *Genome Biol.* **17**, 91 (2016).
43. C. W. Law, Y. Chen, W. Shi, G. K. Smyth, voom: Precision weights unlock linear model analysis tools for RNA-seq read counts. *Genome Biol.* **15**, R29 (2014).
44. O. Alvarez-Garcia, K. M. Fisch, N. E. Wineinger, R. Akagi, M. Saito, T. Sasho, A. I. Su, M. K. Lotz, Increased DNA methylation and reduced expression of transcription factors in human osteoarthritis cartilage. *Arthritis Rheumatol.* **68**, 1876–1886 (2016).
45. K. Benihoud, P. Yeh, M. Perricaudet, Adenovirus vectors for gene delivery. *Curr. Opin. Biotechnol.* **10**, 440–447 (1999).
46. T. C. He, S. Zhou, L. T. da Costa, J. Yu, K. W. Kinzler, B. Vogelstein, A simplified system for generating recombinant adenoviruses. *Proc. Natl. Acad. Sci. U.S.A.* **95**, 2509–2514 (1998).
47. W. C. Russell, Update on adenovirus and its vectors. *J. Gen. Virol.* **81**, 2573–2604 (2000).
48. P. W. Whitlock, T. L. Smith, G. G. Poehling, J. S. Shilt, M. Van Dyke, A naturally derived, cytocompatible, and architecturally optimized scaffold for tendon and ligament regeneration. *Biomaterials* **28**, 4321–4329 (2007).
49. K. J. Stabile, D. Odom, T. L. Smith, C. Northam, P. W. Whitlock, B. P. Smith, M. E. Van Dyke, C. M. Ferguson, An acellular, allograft-derived meniscus scaffold in an ovine model. *Arthroscopy* **26**, 936–948 (2010).
50. J. Lee, J. J. Yoo, A. Atala, S. J. Lee, The effect of controlled release of PDGF-BB from heparin-conjugated electrospun PCL/gelatin scaffolds on cellular bioactivity and infiltration. *Biomaterials* **33**, 6709–6720 (2012).
51. C. Pauli, S. P. Grogan, S. Patil, S. Otsuki, A. Hasegawa, J. Koziol, M. K. Lotz, D. D. D'Lima, Macroscopic and histopathologic analysis of human knee menisci in aging and osteoarthritis. *Osteoarthr. Cartil.* **19**, 1132–1141 (2011).
52. J. Kwok, H. Onuma, M. Olmer, M. K. Lotz, S. P. Grogan, D. D. D'Lima, Histopathological analyses of murine menisci: Implications for joint aging and osteoarthritis. *Osteoarthr. Cartil.* **24**, 709–718 (2016).
53. S. S. Glasson, M. G. Chambers, W. B. Van Den Berg, C. B. Little, The OARSI histopathology initiative—Recommendations for histological assessments of osteoarthritis in the mouse. *Osteoarthritis Cartilage* **18** (suppl. 3), S17–S23 (2010).
54. V. Krenn, L. Morawietz, T. Haupl, J. Neidel, I. Petersen, A. Konig, Grading of chronic synovitis—A histopathological grading system for molecular and diagnostic pathology. *Pathol. Res. Pract.* **198**, 317–325 (2002).

Acknowledgments: We thank L. Creighton, J. Chung, E. Lee, and N. Glembotski for technical assistance. **Funding:** This study was supported by NIH grants AG007996, AG049617, and AR065379. **Author contributions:** M.K.L., K.I.L., and H.A. initiated the investigation of MKX and meniscus, and K.I.L. and J.H. performed MKX cloning. K.I.L., O.A.-G., and S.P.G. performed the in vitro studies of MKX in MSCs and in meniscus cells. K.I.L., J.B., and D.D.D. conducted ex vivo studies with meniscus explants. K.I.L., J.H., and M.O. performed the immunohistochemical and PCR analyses of meniscus. R.G., M.K.L., and A.I.S. performed the RNA-seq studies and GTEx data analysis. K.I.L. and Y.I. performed the surgical meniscus destabilization model in mice. M.K.L. and K.I.L. wrote the manuscript. M.K.L., K.I.L., A.I.S., O.A.-G., D.D.D., and H.A. edited the manuscript. All authors analyzed the data and approved the final manuscript. **Competing interests:** No financial support or other benefits have been obtained from any commercial sources for this study and the authors declare that they have no competing financial interests. **Data and materials availability:** All data associated with this study are present in the paper or the Supplementary Materials.

Submitted 14 February 2019
Resubmitted 6 February 2020
Accepted 21 September 2020
Published 28 October 2020
10.1126/scitranslmed.aan7967

Citation: K. I. Lee, R. Gamini, M. Olmer, Y. Ikuta, J. Hasei, J. Baek, O. Alvarez-Garcia, S. P. Grogan, D. D. D'Lima, H. Asahara, A. I. Su, M. K. Lotz, Mohawk is a transcription factor that promotes meniscus cell phenotype and tissue repair and reduces osteoarthritis severity. *Sci. Transl. Med.* **12**, eaan7967 (2020).